Submitted to Physical Review D

SLAC-PUB-9931

NORDITA-96/18 P

March 1996

hep-ph/9603266

Color-Octet J/ψ Production at Low $p_\perp$

Wai-Keung Tang*

Stanford Linear Accelerator Center, Stanford University, Stanford, CA 94309

M. Vänttinen†

NORDITA, Blegdamsvej 17, DK-2100 Copenhagen

Abstract

We study contributions from color-octet quarkonium formation mechanisms to J/ψ hadroproduction at low $p_\perp$. We include transitions of color-octet $c\bar{c}$ states into "direct" J/ψ and into $\chi_{1,2}$ which decay radiatively into a J/ψ. Together with earlier work, this calculation constitutes a complete analysis of $p_\perp$-integrated J/ψ production at leading twist. We find that the leading-twist contribution is not sufficient to reproduce the observed production rates and polarization of the J/ψ and $\chi_{1,2}$. Hence there must exist other important quarkonium production mechanisms at low $p_\perp$.

Work supported in part by Department of Energy Contract DE-AC03-76SF00515

I. INTRODUCTION

The production and decays of heavy quarkonia have been widely studied using perturbative QCD [1]. Due to the large masses of the c and b quarks, the production or annihilation of heavy-quark–antiquark pairs takes place at a much shorter timescale than the formation of the bound state. This makes it possible to factorize the transition amplitudes. In hadroproduction reactions, also the initial-state hadronic structure is usually expected to be factorizable from the $Q\bar{Q}$ production dynamics in terms of single parton distributions; in other words, quarkonium production is usually taken to be a leading-twist process.

In the simplest approach, one takes the hadroproduction cross section to be a fixed fraction of the integrated $Q\bar{Q}$ cross section below the open heavy flavour threshold. This is called the semilocal duality model or color evaporation model. This model reproduces successfully the dependence of the cross sections on the center-of-mass energy of the collision and on the longitudinal momentum of the quarkonium [2]. However, many observables such as the relative production rates of different charmonium states, transverse momentum distributions, and quarkonium polarization are not predicted. In a more sophisticated approach, a color-singlet $Q\bar{Q}$ pair with the appropriate J^{PC} quantum numbers is produced in the hard process. The quarkonium production amplitude is then written as the convolution of a perturbative amplitude for the production of a $Q\bar{Q}\left[^{2S+1}L_J^{(1)}\right]$ pair (the superscript "(1)" stands for a color-singlet configuration) and a nonrelativistic wave function. This model, in which only the leading, color-singlet Fock component of the quarkonium wave function is taken into account, is called the color singlet model or charmonium model.

In the color singlet model, the polarization of final-state quarkonium is determined by the perturbative dynamics of $Q\bar{Q}$ production and by the angular momentum projection in the wave function. Since polarization is relatively insensitive to higher-order corrections, it provides a very good probe of the basic $Q\bar{Q}$ production mechanisms.

Experimentally, J/ψ polarization has been measured in fixed-target $\pi^- N$ [3–5] and $\bar{p}N$ [5] reactions. The parameter α in the angular distribution $1 + \alpha \cos^2\theta$ of J/ψ decay dileptons

in the Gottfried-Jackson frame has been measured to be $\alpha = 0.028 \pm 0.004$ in $\pi^- N$ reactions and $\alpha = -0.115 \pm 0.061$ in $\bar{p}N$ reactions for longitudinal momentum fraction $x_F > 0$ at 125 GeV [5]. This corresponds to unpolarized production. The theoretical interpretation of these results is complicated by the fact that the "direct" and χ_c-decay components of J/ψ production have not been resolved in the polarization analysis. However, the polarization of the $\psi'(2S)$ has been measured in $\pi^- N$ reactions [6]. The ψ' is also produced unpolarized, with $\alpha = 0.02 \pm 0.14$ for $x_F > 0.25$ at 253 GeV. Apart from an overall normalization factor, the direct J/ψ cross section is expected to be similar to the total ψ' cross section, because no significant contribution to ψ' production from the decays of higher-mass states has been observed. We therefore assume that the direct J/ψ component is unpolarized; the χ-decay component should then also be unpolarized.

In Ref. [7], we calculated the leading-twist contribution to the $p_\perp$-integrated cross section $\sigma(\pi^- N \to J/\psi(\lambda) + X)$, where λ is the helicity of the J/ψ, within the color singlet model. We included contributions from the direct mechanism $gg \to J/\psi + g$ and from the radiative decays of χ_J states produced in the reactions $gg \to \chi_2$, $gg \to \chi_1 g$, $qg \to \chi_1 q$, and $q\bar{q} \to \chi_1 g$. The polarization analysis of the decay contribution is made possible by the electric dipole nature of the decay. In ψ' production, only the direct mechanism needs to be taken into account.

The leading-twist, color-singlet contributions to J/ψ and ψ' production turn out to be dominantly transversely polarized, i.e. $\sigma(\lambda = \pm 1) > \sigma(\lambda = 0)$, with $\alpha \sim 0.5$ for the total J/ψ and $\alpha \sim 0.3$ for the ψ' and direct J/ψ produced by pions. This is in contrast to the experimental observation of unpolarized production. The model also fails to reproduce the observed relative production rates [8] of the J/ψ, χ_1 and χ_2 states. In Ref. [7], we interpreted these discrepancies as evidence for important higher-twist mechanisms of charmonium production.

However, one could argue that the discrepancies are due to neglecting the higher Fock components in the quarkonium wavefunction. These are systematically included in nonrelativistic QCD (NRQCD), an effective field theory which has been formulated during the

recent years [9,10]. NRQCD provides an expansion of quarkonium cross sections and decay widths in terms of the relative velocity v of the heavy quark and antiquark in the bound state. The nonperturbative physics is factorized into an infinite number of matrix elements that scale in a well-defined way in m_Q and v.

Color-octet mechanisms have recently been suggested [11–13] as an explanation of the large quarkonium production rates observed at the Tevatron $p\bar{p}$ collider [14,15]. Some of these rates exceed color-singlet-model predictions by more than an order of magnitude.

There exist color-octet mechanisms of low-$p_\perp$ quarkonium production which are of higher order in v^2 but lower order in α_s compared to the leading color-singlet mechanisms. They might help to reproduce the fixed-target data; the purpose of this paper is to find out whether they do. If not, then the fixed-target discrepancies must be due to a breakdown of the leading-twist approximation of $Q\bar{Q}$ production.

In a recent work [16], we already analyzed the color-octet contribution to ψ' hadroproduction at low $p_\perp$. We found that the leading color-octet contribution is dominantly transversely polarized. Hence, even with the leading color-octet components included, the unpolarized ψ' production data [6] cannot be reproduced. This suggests that there are important higher-twist $Q\bar{Q}$ production mechanisms. The ψ' analysis also applies to the direct component of J/ψ production. In the present paper, we complete our analysis by calculating the contribution to J/ψ production from the radiative decays of χ_1 and χ_2 produced through color-octet intermediate states. It will turn out that this component, too, is dominantly transversely polarized. Furthermore, determinations of color-octet matrix elements from the analysis of other reactions imply that the magnitude of this component is small compared to the data. We shall conclude that in J/ψ as well as in ψ' production, new mechanisms are likely to be important at low $p_\perp$.

II. SUMMARY OF COLOR-SINGLET J/ψ PRODUCTION CROSS SECTIONS

At leading order in α_s and at leading twist, the color-singlet $Q\bar{Q}$ production subprocesses are

$$gg \to {}^1S_0,\ {}^3P_{0,2}, \tag{2.1}$$

$$gg \to {}^3S_1 + g,\ {}^3P_J + g, \tag{2.2}$$

$$gq \to {}^3P_J + q, \tag{2.3}$$

$$q\bar{q} \to {}^3P_J + g, \tag{2.4}$$

i.e. they are obtained from the leading-order annihilation subprocesses such as $J/\psi \to ggg$ by crossing. Note that the process $gg \leftrightarrow {}^3P_1$, with the gluons on mass shell, is forbidden by Yang's theorem [17]. Within the color singlet model, the $Q\bar{Q}$ production mechanism could be different from (2.1–2.4); it could e.g. be a higher-twist process, where many partons from the same initial-state hadron participate in the hard scattering.

The radiative decays $\chi_{1,2} \to J/\psi + \gamma$ are known experimentally to be a major source of J/ψ production. They contribute 30-40% of the total cross section in both pion- and proton-induced reactions [8]. The production of the ψ', on the other hand, is expected to be dominantly due to the direct subprocess (2.2).

The polarization of a ${}^3S_1$ state like the J/ψ is reflected in the polar-angle distribution of its decay dileptons in their rest frame. The parameter α in the angular distribution $1 + \alpha \cos^2\theta$ is related to the polarized J/ψ production cross section

$$\sigma(\lambda) = \sigma_{\rm tot}\ \frac{1 + a\delta_{\lambda 0}}{3 + a}, \tag{2.5}$$

where λ is the helicity of the J/ψ, in the following way:

$$\alpha = \frac{d\sigma(\lambda = 1) - 2d\sigma(\lambda = 0) + d\sigma(\lambda = -1)}{d\sigma(\lambda = 1) + 2d\sigma(\lambda = 0) + d\sigma(\lambda = -1)} = -\frac{a}{2 + a}. \tag{2.6}$$

Because of rotational and parity invariance, $d\sigma(\lambda = 1) = d\sigma(\lambda = -1)$. We work in the Gottfried-Jackson frame, which is defined as the particular quarkonium rest frame where

the beam momentum lies along the z axis and the target momentum lies in the xz plane, with $p_x(\text{target}) \leq 0$. At vanishing transverse momentum of the quarkonium, the Gottfried-Jackson frame is obtained from the laboratory frame by a simple boost, and the choice of the x axis is immaterial.

We analyzed the polarized cross sections of J/ψ production through the direct process and χ_J decays in Ref. [7], where we found that the color singlet model is insufficient to explain the existing fixed-target data. In the color singlet model, the χ_1 and direct J/ψ cross sections are predicted to be significantly lower than measured relative to the χ_2 cross section, which is within a factor $K = 2$–3 of the experimental value. In contrast with the observed unpolarized production, the predicted total J/ψ cross section is dominantly transversely polarized even if the various contributions are renormalized according to the data. The quantitative results of the calculation of Ref. [7] are listed in Table I together with experimental data and color-octet predictions.

III. COLOR-OCTET J/ψ PRODUCTION CROSS SECTIONS

As one calculates quarkonium production cross sections within the NRQCD factorization scheme, one is using two expansions: the perturbative expansion of the short-distance $Q\bar{Q}$ production amplitude and the velocity expansion of the long-distance quarkonium formation amplitude. General rules for finding out the power dependence of the NRQCD matrix elements on m_Q and v can be found in Refs. [9,10]. At leading order in perturbation theory, i.e. $O(\alpha_s^2)$, and up to next-to-leading order in the velocity expansion, the subprocesses for leading-twist J/ψ production through color-octet intermediate states are

$$q\bar{q} \to c\bar{c}\left[{}^3S_1^{(8)}\right] \to J/\psi + gg, \tag{3.1}$$

$$gg \to c\bar{c}\left[{}^1S_0^{(8)}\right] \to J/\psi + g, \tag{3.2}$$

$$gg \to c\bar{c}\left[{}^3P_J^{(8)}\right] \to J/\psi + g, \tag{3.3}$$

$$q\bar{q} \to c\bar{c}\left[{}^3S_1^{(8)}\right] \to \chi_J + g \to J/\psi + \gamma + g. \tag{3.4}$$

These are illustrated by the Feynman diagrams of Fig. 1, where the blob represents a nonperturbative transition. Their cross sections are proportional to the NRQCD matrix elements

$$\langle 0|\mathcal{O}_8^{J/\psi}(^3S_1)|0\rangle \sim m_c^3 v^7, \tag{3.5}$$

$$\langle 0|\mathcal{O}_8^{J/\psi}(^1S_0)|0\rangle \sim m_c^3 v^7, \tag{3.6}$$

$$\langle 0|\mathcal{O}_8^{J/\psi}(^3P_J)|0\rangle \sim m_c^5 v^7, \tag{3.7}$$

$$\langle 0|\mathcal{O}_8^{\chi_J}(^3S_1)|0\rangle \sim m_c^3 v^5, \tag{3.8}$$

respectively. Hence the direct J/ψ production cross sections are proportional to $\alpha_s^2 v^7$, and the χ_J cross section is proportional to $\alpha_s^2 v^5$. They are to be compared with the leading color-singlet cross sections

$$\begin{aligned} \sigma(gg \to \chi_2) &\sim \alpha_s^2 v^5, \\ \sigma(gg \to J/\psi + g) &\sim \alpha_s^3 v^3, \\ \sigma(ij \to \chi_1 + k) &\sim \alpha_s^3 v^5. \end{aligned} \tag{3.9}$$

The amplitude

$$A\left(q\bar{q} \to c\bar{c}\left[^3P_J^{(8)}\right] \to J/\psi + g\right) \tag{3.10}$$

is of higher order in v^2 than the amplitudes of the processes (3.1–3.4), because the lowest-order non-perturbative transition (single chromoelectric dipole) is forbidden by charge conjugation. Furthermore, the amplitude

$$A\left(gg \to c\bar{c}\left[^3S_1^{(8)}\right] \to \chi_J + g\right) \tag{3.11}$$

is of higher order in α_s because the amplitude $A\left(gg \to c\bar{c}\left[^3S_1^{(8)}\right]\right)$ vanishes in the leading order. Charge conjugation or Yang's theorem would not require this amplitude to vanish because the $c\bar{c}$ pair is not in a color-singlet state.

The contribution to $\sigma(hN \to J/\psi(\lambda) + X)$ from the direct production subprocesses (3.1–3.3) follows immediately from the ψ' production analysis of Ref. [16]:

$$\sigma_{\rm octet}(hN \to \text{direct } J/\psi(\lambda) + X) = O_1\langle 0|\mathcal{O}_8^{J/\psi}(\,^3P_1)|0\rangle(3-2\delta_{\lambda 0}) + O_2\langle 0|\mathcal{O}_8^{J/\psi}(\,^1S_0)|0\rangle(1-\delta_{\lambda 0}) + O_3\langle 0|\mathcal{O}_8^{J/\psi}(\,^3S_1)|0\rangle(1-\delta_{\lambda 0}). \tag{3.12}$$

The coefficients are

$$O_1 = \frac{5\pi^3\alpha_s^2}{9M^7}\,\Phi_{gg/hN}(M^2/s,\mu_F), \tag{3.13}$$

$$O_2 = \frac{5\pi^3\alpha_s^2}{24M^5}\,\Phi_{gg/hN}(M^2/s,\mu_F), \tag{3.14}$$

$$O_3 = \frac{8\pi^3\alpha_s^2}{27M^5}\,\sum_q \left[\Phi_{q\bar{q}/hN}(M^2/s,\mu_F) + \Phi_{\bar{q}q/hN}(M^2/s,\mu_F)\right], \tag{3.15}$$

where

$$\Phi_{ij/hN}(\tau,\mu_F) \equiv \int dx_1 dx_2\; f_{i/h}(x_1,\mu_F)\; f_{j/N}(x_2,\mu_F)\;\delta\left(1-\frac{\tau}{x_1x_2}\right) \tag{3.16}$$

is a parton flux factor evaluated at the leading-twist factorization scale μ_F (since the final-state gluons are taken to be soft, the kinematics is essentially that of a $2 \to 1$ subprocess, with $\hat{s} = M^2 = 4m_c^2$). For ease of reference, we plot in Fig. 2 the gg and $q\bar{q}$ flux factors in π^--proton, proton-proton and antiproton-proton collisions using the GRV-LO parton distributions [18]. In accordance with the existing experiments, the integral is over the region $x_F = x_1 - x_2 > 0$.

The polarization of the directly produced J/ψ has not been measured separately from the polarization of those from χ decays. However, the fact that the ψ' are produced unpolarized [6] lets us expect that the direct J/ψ component is also unpolarized. Then, as in the ψ' case, only about half of the observed direct production can be due to the strongly transversely polarized contribution (3.12). We discussed the derivation of a quantitative bound on a linear combination of NRQCD matrix elements in Ref. [16].

To evaluate the contribution from the process (3.4), we make use of the fact that both the $c\bar{c}\left[^3S_1^{(8)}\right] \to \chi_J + g$ transition and the radiative decay of the χ_J are electric dipole transitions. The necessary formulas are given in the appendix. From the $q\bar{q} \to c\bar{c}$ scattering amplitude,

$$\mathcal{O}^{AB}_{q\bar{q}\to c\bar{c}} = \frac{4\pi\alpha_s}{(p_{\bar{q}}+p_q)^2}\;\bar{v}_C(p_{\bar{q}})\;\gamma_\mu T^a_{CD}\;u_D(p_q)\;T^{AB}_a\gamma^\mu, \tag{3.17}$$

we derive

$$\overline{\sum_a}\left|A\left(q\bar{q}\to c\bar{c}\left[{}^3S_1^{(8)};S_z,a\right]\right)\right|^2 = \frac{32\pi^2\alpha_s^2}{9}\;(1-\delta_{S_z0})\,. \tag{3.18}$$

The subprocess cross sections then become

$$\begin{aligned}
&\sigma\left(q\bar{q}\to c\bar{c}\left[{}^3S_1^{(8)}\right]\to\chi_1+g\to J/\psi(\lambda)+\gamma+g\right)\\
&=\frac{16\pi^3\alpha_s^2}{27M^5}\;\delta\left(1-\frac{M^2}{\hat{s}}\right)\mathrm{Br}\left(\chi_1\to J/\psi+\gamma\right)\left\langle 0\left|\mathcal{O}_8^{\chi_1}({}^3S_1)\right|0\right\rangle\frac{3-\delta_{\lambda 0}}{8},
\end{aligned}\tag{3.19}$$

$$\begin{aligned}
&\sigma\left(q\bar{q}\to c\bar{c}\left[{}^3S_1^{(8)}\right]\to\chi_2+g\to J/\psi(\lambda)+\gamma+g\right)\\
&=\frac{16\pi^3\alpha_s^2}{27M^5}\;\delta\left(1-\frac{M^2}{\hat{s}}\right)\mathrm{Br}\left(\chi_2\to J/\psi+\gamma\right)\left\langle 0\left|\mathcal{O}_8^{\chi_2}({}^3S_1)\right|0\right\rangle\frac{47-21\delta_{\lambda 0}}{120}.
\end{aligned}\tag{3.20}$$

Using the NRQCD result $\langle 0|\mathcal{O}_8^{\chi_2}({}^3S_1)|0\rangle = (5/3)\,\langle 0|\mathcal{O}_8^{\chi_1}({}^3S_1)|0\rangle$, valid up to corrections of relative order v^2, we arrive at

$$\begin{aligned}
&\sigma_{\mathrm{octet}}(hN\to\chi_J+g\to J/\psi(\lambda)+\gamma+g)\\
&=\sum_q\left[\Phi_{q\bar{q}/hN}\left(\frac{M^2}{s},\mu_F\right)+\Phi_{\bar{q}q/hN}\left(\frac{M^2}{s},\mu_F\right)\right]\;\frac{16\pi^3\alpha_s^2}{27M^5}\;\langle 0|\mathcal{O}_8^{\chi_1}({}^3S_1)|0\rangle\\
&\quad\times\left[\mathrm{Br}\left(\chi_1\to J/\psi+\gamma\right)\frac{3-\delta_{\lambda 0}}{8}\;+\;\frac{5}{3}\,\mathrm{Br}\left(\chi_2\to J/\psi+\gamma\right)\frac{47-21\delta_{\lambda 0}}{120}\right].
\end{aligned}\tag{3.21}$$

Our expressions for the polarized cross sections, eqs. (3.12, 3.21), agree with the unpolarized cross sections given in Refs. [13,19].

Each of the two components in eq. (3.21) alone would correspond to $\alpha = 0.2$ and $\alpha = 0.29$ in the decay angular distribution of the J/ψ, respectively. Hence this contribution, similarly to the color-singlet contribution [7] and the direct color-octet contribution of eq. (3.12), is dominantly transversely polarized. Because J/ψ production in πN reactions is observed to be unpolarized, one is again led to conclude that there are important $c\bar{c}$ production mechanisms beyond leading twist.

The value of the $\langle 0|\mathcal{O}_8^{\chi_1}({}^3S_1)|0\rangle$ matrix element has been obtained from the analysis of CDF data at large $p_\perp$ [12,13] and of B decays into P-wave charmonium [11,20]. These

values actually imply that the contribution (3.21) is rather small compared to the observed J/ψ cross section. Using $\langle 0|\mathcal{O}_8^{\chi_1}(^3S_1)|0\rangle = (9.8 \pm 1.3) \cdot 10^{-3}$ (GeV)^3 [13], $\alpha_s = 0.26$ and $M = 3.5$ GeV, we obtain

$$\begin{aligned}
&\sum_\lambda \sigma_{\rm octet}(hN \to \chi_{1,2} + g \to J/\psi(\lambda) + \gamma + g) \\
&= 4.5 \text{ nb} \sum_q \left[\Phi_{q\bar{q}/hN}\left(\frac{M^2}{s}, \mu_F\right) + \Phi_{\bar{q}q/hN}\left(\frac{M^2}{s}, \mu_F\right)\right] = \begin{cases} 1.3 \text{ nb } (\pi^- \text{ beam}) \\ 0.6 \text{ nb } (p \text{ beam}) \end{cases}
\end{aligned} \tag{3.22}$$

at $E_{\rm lab}(\pi) = 300$ GeV. These numbers are more than an order of magnitude smaller than the experimental cross sections of 72 nb, 67 nb and 45 nb (with errors of about 25%) for π^+, π^- and p beams, respectively [8]. Hence the color-octet mechanisms cannot reproduce the fixed-target data. On the other hand, our analysis does not set any constraints that would contradict the color-octet description of other reactions.

IV. SUMMARY

In this paper, we have considered the production of J/ψ charmonium in fixed-target reactions within the factorization scheme of nonrelativistic QCD (NRQCD) [10]. We have calculated the contribution from the radiative decays, $\chi_{1,2} \to J/\psi + \gamma$, of χ_J charmonia produced through intermediate color-octet $c\bar{c}$ states at leading twist. The "direct" color-octet component of J/ψ production is given by our analysis of color-octet ψ' production [16]. Together with our earlier evaluation of the color-singlet component [7], the present calculation constitutes a complete analysis of leading-twist J/ψ production at low $p_\perp$. We have included contributions from nonperturbative transitions between intermediate $c\bar{c}$ states and charmonium up to relative order v^4, where v is the relative velocity of the charm quark and antiquark in the bound state. The $c\bar{c}$ production amplitudes have in each case been evaluated at the lowest order in α_s allowed by the quantum numbers of the intermediate $c\bar{c}$ state.

The results on J/ψ production obtained in this paper and Refs. [7,16] have been collected

in Table I. In the evaluation of color-octet contributions, we have used the NRQCD matrix elements determined in Refs. [13,21].

Our motivation has been to test both the NRQCD picture of the long-distance quarkonium formation process and the leading-twist approximation of short-distance $Q\bar{Q}$ production. Predictions of the final-state charmonium polarization provide a very good test of the models involved. They are relatively insensitive to higher-order corrections in perturbation theory. Polarization analysis of the long-distance process is made possible by the fact that the emission or absorption of soft gluons does not change the heavy quark spins.

We have shown that the leading-twist contribution to J/ψ production is dominantly transversely polarized, i.e. $\alpha > 0$ in the angular distribution, $1 + \alpha \cos^2\theta$, of the decay $J/\psi \to \ell^+\ell^-$ in the Gottfried-Jackson frame. Actually, all but one of the individual components of the theoretical cross section are dominantly transversely polarized. The only exception is the small contribution from the radiative decay of the χ_1 produced by color-singlet mechanisms, which gives $\alpha \approx -0.15$. Experimentally, on the other hand, it has been observed that S-wave charmonia are produced unpolarized.

Furthermore, the values of NRQCD matrix elements determined from other reactions imply that the normalization of color-octet contributions is small compared to the observed charmonium cross sections.

Assuming that the NRQCD factorization scheme provides a complete description of quarkonium formation, the reason for the discrepancies must lie in the choice of $c\bar{c}$ production mechanisms. Hence there should exist important higher-twist mechanisms of $c\bar{c}$ production at small $p_\perp$.

Since the mass of the b quark is significantly larger than the c quark mass, all the approximations involved in the calculation – perturbation theory, the velocity expansion, and the leading-twist approximation – are expected to work better for bottomonium. Unfortunately, the existing bottomonium production data is insufficient to test our predictions.

APPENDIX A: DIPOLE TRANSITIONS

1. Electric dipole transitions

The polarized cross section of J/ψ production via the radiative decay of a χ_J charmonium state is

$$\begin{aligned}
&\sigma\left(ij \to \chi_J + X \to J/\psi(\lambda) + \gamma + X\right) \\
&= \frac{1}{2\hat{s}} \int \mathrm{dLips}(J/\psi, \gamma, X) \overline{\sum} \left|A\left(ij \to \chi_J + X \to J/\psi(\lambda) + \gamma + X\right)\right|^2 \\
&= \frac{1}{2\hat{s}} \int \frac{dp^2(\chi_J)}{2\pi}\, \mathrm{dLips}(\chi_J, X)\, \mathrm{dLips}(J/\psi, \gamma) \overline{\sum} \left|A\right|^2, \qquad \text{(A1)}
\end{aligned}$$

where $\hat{s} = (p_i + p_j)^2$ is the invariant mass of the initial state and λ is the helicity of the J/ψ. In the limit where the momenta of the photon and final-state light hadrons are neglected, it equals the z component of the spin of the J/ψ. The transition amplitude is

$$\begin{aligned}
&A\left(ij \to \chi_J + X \to J/\psi(\lambda) + \gamma(\mu) + X\right) \\
&= \sum_{J_z} A\left(ij \to \chi_J(J_z) + X\right)\ \varphi(\chi_J)\ A\left(\chi_J(J_z) \to J/\psi(\lambda) + \gamma(\mu)\right), \qquad \text{(A2)}
\end{aligned}$$

where $\varphi(\chi_J)$ is the propagator of the χ_J and μ is the helicity of the photon. In the limit of small χ_J decay width,

$$\lim_{\Gamma_{\mathrm{tot}}(\chi_J)\to 0} \varphi(\chi_J)\varphi^*(\chi_J) = \frac{\pi}{M_{\chi_J}\Gamma_{\mathrm{tot}}(\chi_J)} \delta(M_{\chi_J}^2 - p_{\chi_J}^2). \qquad \text{(A3)}$$

In the electric dipole approximation, the χ_J decay amplitude is written as

$$\begin{aligned}
A\left(\chi_J(J_z) \to J/\psi(\lambda) + \gamma(\mu)\right) &= \sum_{L_z S_z} \langle J J_z | L_z S_z \rangle\, A\left(c\bar{c}(L_z, S_z) \to J/\psi(\lambda) + \gamma(\mu)\right) \\
&= \sum_{L_z S_z} \langle J J_z | L_z S_z \rangle N \delta_{S_z \lambda} \epsilon^*_{L_z}(\mu) \\
&= N \langle J J_z | J_z - \lambda, \lambda \rangle \epsilon^*_{J_z - \lambda}(\mu), \qquad \text{(A4)}
\end{aligned}$$

where the symbol $\delta_{S_z\lambda}$ expresses the heavy quark spin conservation and the normalization factor is

$$N = \left(\frac{24\pi M_{J/\psi} M_{\chi_J}^2 \Gamma(\chi_J \to J/\psi + \gamma)}{M_{\chi_J}^2 - M_{J/\psi}^2} \right)^{1/2}. \qquad \text{(A5)}$$

Using the results

$$\mathrm{dLips}(J/\psi,\gamma) = \frac{M_{\chi_J}^2 - M_{J/\psi}^2}{32\pi^2 M_{J/\psi} M_{\chi_J}^2}\, d\Omega, \tag{A6}$$

$$\sum_\mu \int d\Omega\, \epsilon_i(\mu)\epsilon_j^*(\mu) = \frac{8\pi}{3}\delta_{ij}, \tag{A7}$$

where $d\Omega$ is a solid angle element in the charmonium rest frame, we obtain

$$\begin{aligned}
&\sigma(ij \to \chi_J + X \to J/\psi(\lambda) + \gamma + X) \\
&= \mathrm{Br}\,(\chi_J \to J/\psi + \gamma) \sum_{J_z} |\langle JJ_z|J_z - \lambda, \lambda\rangle|^2 \frac{1}{2\hat{s}} \int \mathrm{dLips}(\chi_J, X) \overline{\sum} |A(ij \to \chi_J(J_z) + X)|^2 \\
&= \mathrm{Br}\,(\chi_J \to J/\psi + \gamma) \sum_{J_z} |\langle JJ_z|J_z - \lambda, \lambda\rangle|^2\, \sigma(ij \to \chi_J(J_z) + X).
\end{aligned} \tag{A8}$$

This result was also used in the color-singlet-model calculation of Ref. [7].

2. Chromoelectric dipole transitions

Analogously with eq. (A8), we write the cross section of χ_J production via the chromoelectric dipole "decay" of a color-octet $c\bar{c}\,[^3S_1]$ state as

$$\begin{aligned}
\sigma\left(ij \to c\bar{c}\left[^3S_1^{(8)}\right] \to \chi_J(J_z) + g\right) &= \frac{1}{8(2J+1)m_c} \langle 0|\mathcal{O}_8^{\chi_J}(^3S_1)|0\rangle \sum_{S_z} |\langle JJ_z|J_z - S_z, S_z\rangle|^2 \\
&\quad \times \frac{\pi}{M^4}\, \delta\left(1 - \frac{M^2}{\hat{s}}\right) \overline{\sum_a}\, \left|A\left(ij \to c\bar{c}\left[^3S_1^{(8)}; S_z, a\right]\right)\right|^2,
\end{aligned} \tag{A9}$$

where $\langle 0|\mathcal{O}_8^{\chi_J}(^3S_1)|0\rangle$ is a matrix element of nonrelativistic QCD and

$$A\left(ij \to c\bar{c}\left[^3S_1^{(8)}, S_z, a\right]\right) = \sqrt{2}\, T_{AB}^a\, \mathrm{Tr}\left[\mathcal{O}_{ij\to c\bar{c}}^{AB} \frac{\not{\epsilon}^*(S_z)(\not{P} + M)}{2\sqrt{2}}\right]. \tag{A10}$$

$\mathcal{O}_{ij\to c\bar{c}}^{AB}$ is the amplitude for the perturbative process $ij \to c\bar{c}$, as given by Feynman rules (A, B are the color indices of the heavy quark and antiquark; the heavy-quark and antiquark spinors are truncated), and $M = 2m_c$ is the mass of the $c\bar{c}$ state. Combining eqs. (A8) and (A9), we have the final result

$$
\begin{aligned}
&\sigma\left(ij \to c\bar{c}\left[{}^3S_1^{(8)}\right] \to \chi_J + g \to J/\psi(\lambda) + \gamma + g\right) \\
&= \mathrm{Br}\left(\chi_J \to J/\psi + \gamma\right) \frac{1}{8(2J+1)m_c} \langle 0|\mathcal{O}_8^{\chi_J}({}^3S_1)|0\rangle \sum_{J_z} |\langle JJ_z|J_z - \lambda, \lambda\rangle|^2 \\
&\quad \times \sum_{S_z} |\langle JJ_z|J_z - S_z, S_z\rangle|^2 \frac{\pi}{M^4}\, \delta\left(1 - \frac{M^2}{\hat{s}}\right) \overline{\sum_a} \left|A\left(ij \to c\bar{c}\left[{}^3S_1^{(8)}; S_z, a\right]\right)\right|^2 . \qquad \text{(A11)}
\end{aligned}
$$

REFERENCES

* Work supported in part by Department of Energy contract DE–AC03–76SF00515 and DE–AC02–76ER03069.

† Work supported in part by the Academy of Finland under project number 8579.

[1] For a review, see e.g. G. A. Schuler, Report No. CERN-TH.7170/94, hep-ph/9403387, to appear in Phys. Rep.

[2] A recent comparison of the model predictions with data is given by R. Gavai *et al.*, Int. J. Mod. Phys. A **10**, 3043 (1995).

[3] J. Badier *et al.*, Z. Phys. C **20**, 101 (1983).

[4] C. Biino *et al.*, Phys. Rev. Lett. **58**, 2523 (1987).

[5] E537 Collaboration, C. Akerlof *et al.*, Phys. Rev. D **48**, 5067 (1993).

[6] J. G. Heinrich *et al.*, Phys. Rev. D **44**, 1909 (1991).

[7] M. Vänttinen, P. Hoyer, S. J. Brodsky and Wai-Keung Tang, Phys. Rev. D **51**, 3332 (1995).

[8] E705 Collaboration, L. Antoniazzi *et al.*, Phys. Rev. Lett. **70**, 383 (1993).

[9] G. P. Lepage *et al.*, Phys. Rev. D **46**, 4052 (1992).

[10] G. T. Bodwin, E. Braaten, and G. P. Lepage, Phys. Rev. D **51**, 1125 (1995).

[11] E. Braaten and S. Fleming, Phys. Rev. Lett. **74**, 3327 (1995).

[12] P. Cho and A. K. Leibovich, Phys. Rev. D **53**, 150 (1996).

[13] P. Cho and A. K. Leibovich, Report No. CALT-68-2026, hep-ph/9511315, to appear in Phys. Rev. D.

[14] CDF Collaboration, F. Abe *et al.*, Phys. Rev. Lett. **75**, 4358 (1995); CDF Collaboration,

V. Papadimitriou *et al.*, Report No. Fermilab-Conf-95/128-E, presented at 30th Rencontres de Moriond: *QCD and High Energy Hadronic Interactions*, Meribel les Allues, France, March 1995.

[15] D0 Collaboration, S. Abachi *et al.*, Reports No. Fermilab-Conf-95/205-E and Fermilab-Conf-95/206-E, submitted to International Europhysics Conference on High Energy Physics (HEP 95), Brussels, Belgium, July-August 1995.

[16] Wai-Keung Tang and M. Vänttinen, Report No. SLAC-PUB-95-6931 (1995), hep-ph/9506378, to appear in Phys. Rev. D. Note that the notation in the preprint version was inconsistent with that of other authors and will be changed in the published version.

[17] C. N. Yang, Phys. Rev. **77**, 242 (1950).

[18] M. Glück, E. Reya and A. Vogt, Z. Phys. **C53**, 127 (1992); *ibid.* 651.

[19] S. Fleming and I. Maksymyk, Report No. MADPH-95-922, hep-ph/9512320.

[20] G. T. Bodwin, E. Braaten, T. C. Yuan, and G. P. Lepage, Phys. Rev. D **46**, 3703 (1992).

[21] J. Amundson, S. Fleming and I. Maksymyk, Report No. UTTG-10-95, hep-ph/9601298.

FIGURES

FIG. 1. The Feynman diagrams which describe the leading color-octet mechanisms of J/ψ and χ_J production. The blob represents a nonperturbative transition. The dashed line indicates the color-octet intermediate state.

FIG. 2. Gluon-gluon and quark-antiquark flux factors, Φ_{gg} and $\sum_q(\Phi_{q\bar{q}} + \Phi_{\bar{q}q})$, plotted as a function of $\tau = \hat{s}/s = x_1 x_2$ using the GRV-LO parton distributions [18]. (a) π^--proton reactions, (b) proton-proton reactions, (c) antiproton-proton reactions. Solid line: $\Phi_{gg}(\mu_F = M)$. Dotted line: $\Phi_{gg}(\mu_F = M/2)$. Dashed line: $\sum_q [\Phi_{q\bar{q}} + \Phi_{\bar{q}q}] (\mu_F = M)$. Dash-dotted line: $\sum_q [\Phi_{q\bar{q}} + \Phi_{\bar{q}q}] (\mu_F = M/2)$. We used $M = 3.5$ GeV.

TABLES

TABLE I. Leading-twist color-singlet and color-octet contributions to J/ψ production in $\pi^- N$ collisions at 300 GeV shown together with experimental data [5,8]. The cross sections have been integrated over $x_F > 0$ and normalized by $\sigma_{\rm exp}(\text{all } J/\psi) = 178 \pm 21$ nb. The dependence of theoretical contributions on the strong coupling constant α_s and on the relative velocity v of the quark and antiquark in the bound state is indicated. We used the GRV-LO parton distributions [18].

Observed process theoretical subprocesses	Scaling	$\sigma/\sigma_{\rm exp}(\text{all } J/\psi)$	α
$\pi^- N \to \chi_2 \to J/\psi + \gamma$		0.143 ± 0.020	
$gg \to \chi_2$	$\alpha_s^2 v^5$	0.059	1.0[a]
$q\bar{q} \to {}^3S_1^{(8)} \to \chi_2$	$\alpha_s^2 v^5$	0.0041[b]	0.29
$\pi^- N \to \chi_1 \to J/\psi + \gamma$		0.201 ± 0.024	
$q\bar{q} \to \chi_1 g$	$\alpha_s^3 v^5$	0.0016	0.19
$qg \to \chi_1 q$	$\alpha_s^3 v^5$	0.0029	-0.22
$gg \to \chi_1 g$	$\alpha_s^3 v^5$	0.0035	-0.27
$q\bar{q} \to {}^3S_1^{(8)} \to \chi_1$	$\alpha_s^2 v^5$	0.0034[b]	0.2
$\pi^- N \to$ direct J/ψ		0.56 ± 0.03	
$gg \to J/\psi + g$	$\alpha_s^3 v^3$	0.072	0.26
$gg \to {}^3P_J^{(8)} \to J/\psi$	$\alpha_s^3 v^7$	0.16[c]	0.5
$gg \to {}^1S_0^{(8)} \to J/\psi$	$\alpha_s^3 v^7$		1.0
$q\bar{q} \to {}^3S_1^{(8)} \to J/\psi$	$\alpha_s^3 v^7$	0.020[b]	1.0
$\pi^- N \to$ all J/ψ		1	0.028 ± 0.004

[a]Reduced to $\alpha \approx 0.85$ if transverse momentum smearing is taken into account [7].

[b]Using the color-octet matrix elements of Ref. [13].

[c]Combined contribution from ${}^3P_J^{(8)}$ and ${}^1S_0^{(8)}$ intermediate states, using the linear combination of color-octet matrix elements determined in Ref. [21].

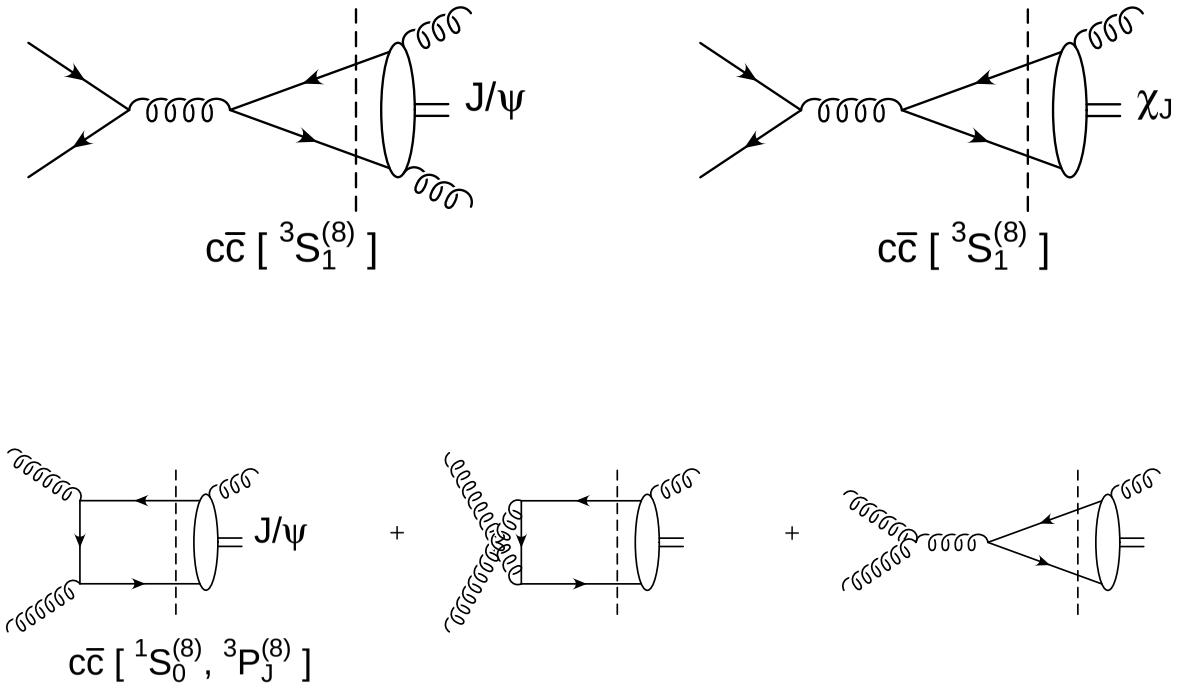

Fig. 1

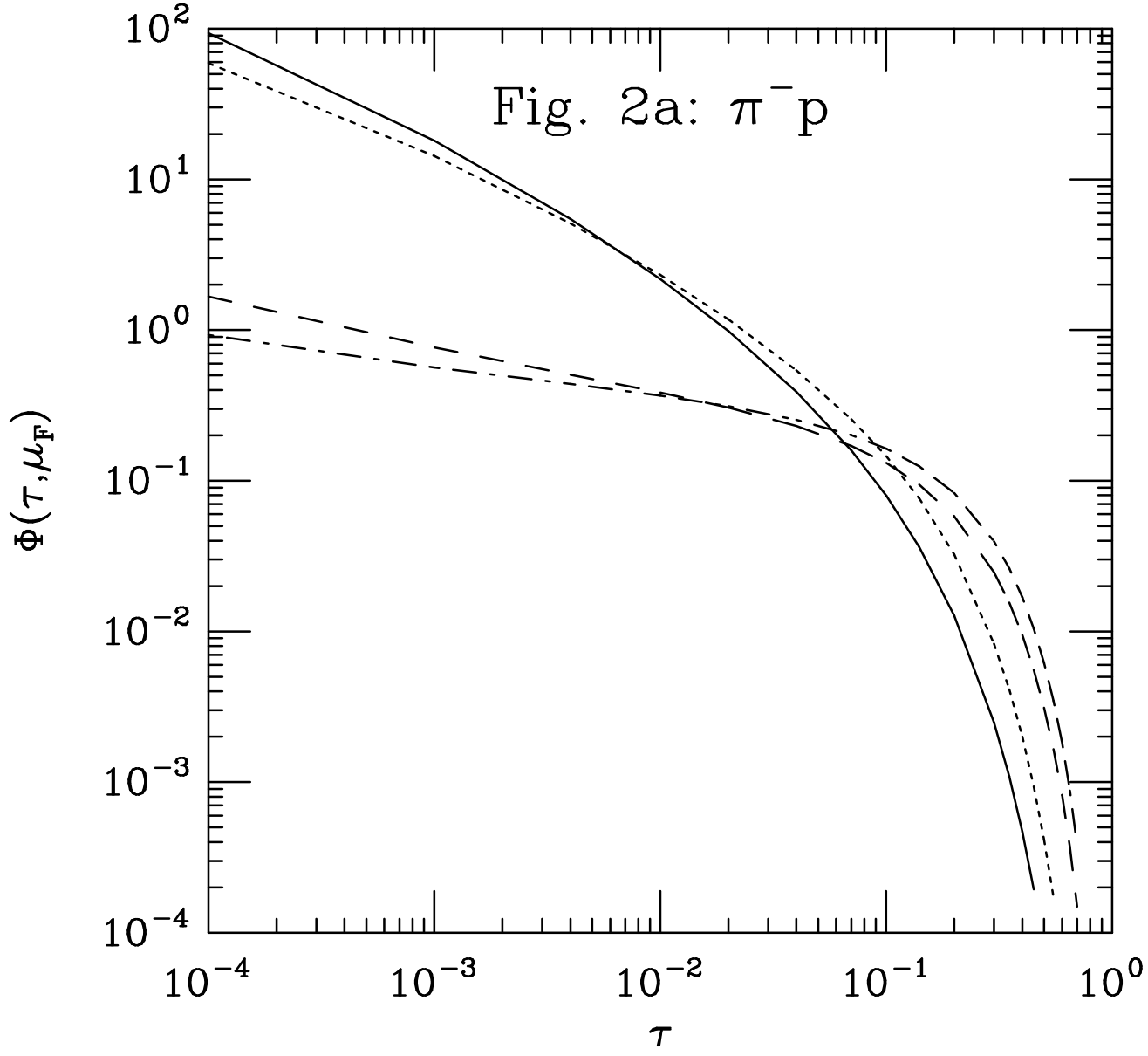
Fig. 2a: $\pi^- p$
10^2
10^1
10^0
10^{-1}
10^{-2}
10^{-3}
10^{-4}
$\Phi(\tau,\mu_F)$
10^{-4}
10^{-3}
10^{-2}
10^{-1}
10^0
τ

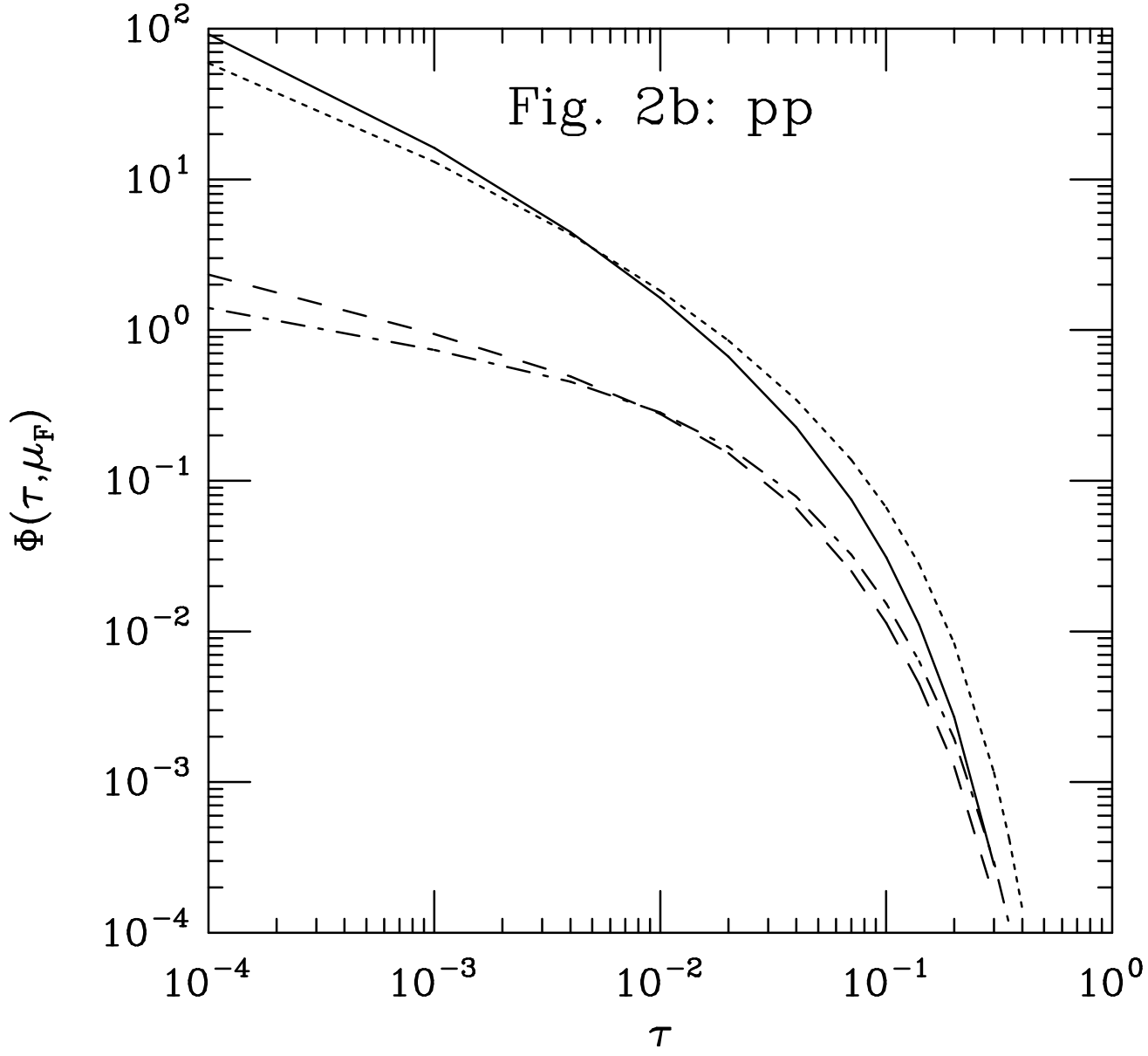
Fig. 2b: pp
10^2
10^1
10^0
10^{-1}
10^{-2}
10^{-3}
10^{-4}
$\Phi(\tau,\mu_F)$
10^{-4}
10^{-3}
10^{-2}
10^{-1}
10^0
τ

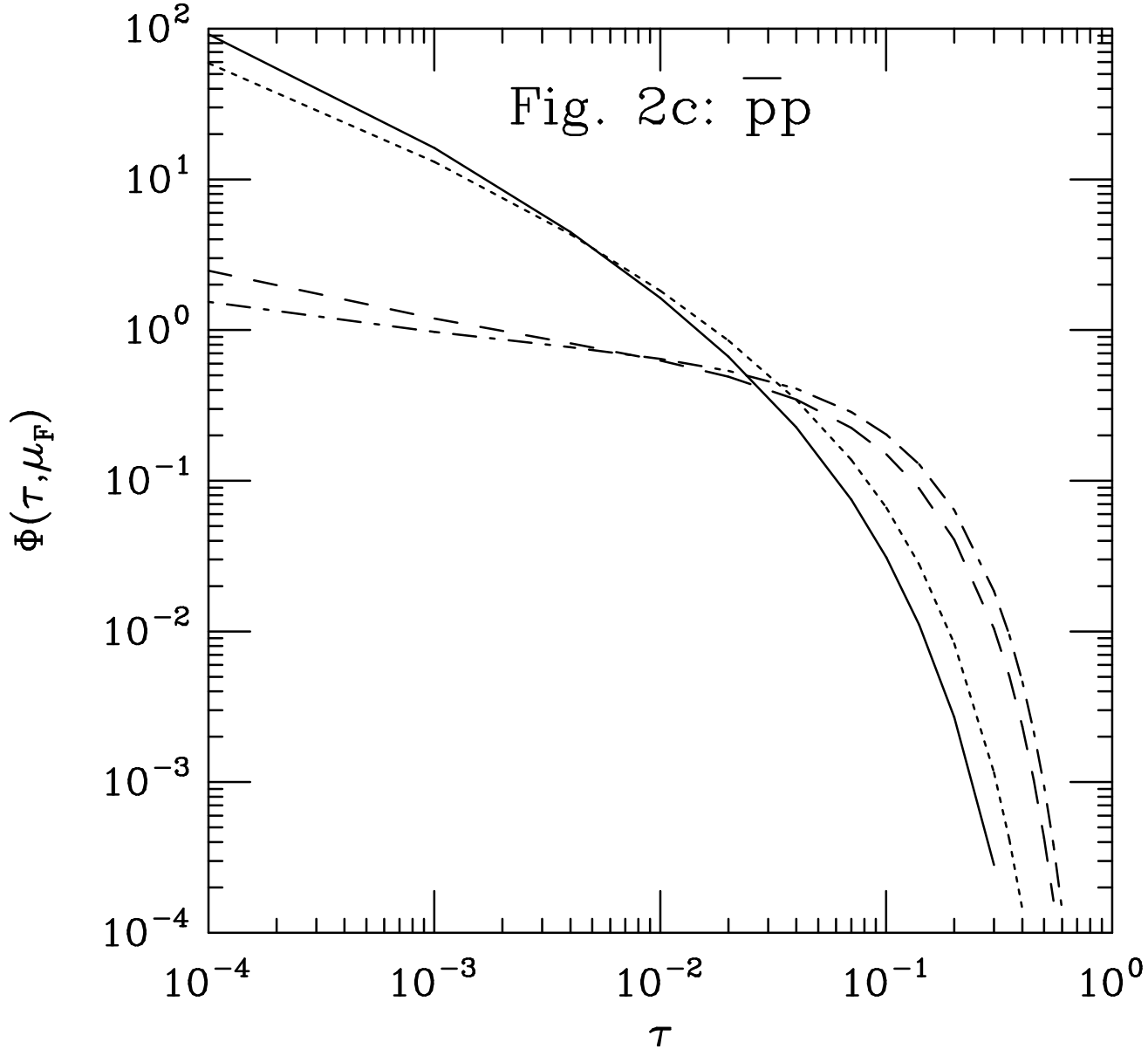
Fig. 2c: $\overline{\mathrm{p}}\mathrm{p}$
10^2
10^1
10^0
10^{-1}
10^{-2}
10^{-3}
10^{-4}
$\Phi(\tau,\mu_F)$
10^{-4}
10^{-3}
10^{-2}
10^{-1}
10^0
τ